Environmental Modelling and Software 175 (2024) 105995

Contents lists available at ScienceDirect

Environmental Modelling and Software

journal homepage: www.elsevier.com/locate/envsoft

Nature-inspired optimal tuning of input membership functions of fuzzy inference system for groundwater level prediction

Vipul Bhadani [a,1], Abhilash Singh [a,1], Vaibhav Kumar [b,*], Kumar Gaurav [a,*]

[a] Department of Earth and Environmental Sciences, Indian Institute of Science Education and Research Bhopal, Bypass road, Bhopal, 462066, Madhya Pradesh, India

[b] Department of Data Science and Engineering, Indian Institute of Science Education and Research Bhopal, Bypass road, Bhopal, 462066, Madhya Pradesh, India

ARTICLE INFO

Keywords:
Fuzzy inference system
Invasive weed optimization
Groundwater level
Machine learning

ABSTRACT

We present a novel regression algorithm that combines a Fuzzy Inference System (FIS) with a nature-inspired algorithm to predict variations in GroundWater Levels (GWLs). Initially, we considered several input features, including precipitation, temperature, evaporation, relative humidity, soil type, and GWL Lag. A feature importance analysis using regression tree ensemble learning reveals GWL lag as the most relevant feature and soil type as the least relevant. We eliminate features with low importance scores (soil type, temperature, and evaporation) to improve the computational efficiency. Our approach leverages Fuzzy C-Means (FCM) clustering to develop a Sugeno-type FIS with definite clusters. The dataset is clustered based on feature similarity, and Gaussian membership functions are assigned to each cluster. The mapping of each point is controlled by the range and standard deviation of the Gaussian membership functions. We train the model keeping 70% of the dataset, iteratively tuning the parameters of the Gaussian membership function for all clusters through the Invasive Weed Optimization (IWO) algorithm. The performance of the model is then evaluated using the remaining 30% of the datasets.

The F-IWO-GWL model accurately predicts GWL fluctuations, achieving a high correlation coefficient (R = 0.89), low normalized root mean square error (nRMSE = 0.18), and minimal bias (bias = 0.08). A comparative analysis involving seventeen benchmark algorithms reveals the superior performance of our algorithm. To ensure a fair comparison, we calculated key metrics including Akaike's Information Criterion (AIC), Bayesian Information Criterion (BIC), and Corrected AIC (AICc). The F-IWO-GWL algorithm exhibits the lowest values for AIC, BIC, and AICc among all tested algorithms, suggesting the best goodness-of-fit. This study provides a robust approach for predicting GWL fluctuation, applicable to various groundwater management scenarios. It offers valuable insights for policymakers and stakeholders involved in groundwater management, aiding informed decision-making.

1. Introduction

Groundwater is an important resource crucial for sustaining life on Earth. In recent years, the availability of groundwater supplies has come under imminent pressure due to the swift pace of urbanization and population growth (Niranjannaik et al., 2022). Furthermore, the rapid increase in anthropogenic activities has led to the over-exploitation of groundwater (Zhongming et al., 2021). The situation is particularly alarming in arid and semi-arid regions. Consequently, effective groundwater management and integrated planning are crucial in meeting present and future water demand (Maiti and Tiwari, 2014). The groundwater level dynamics are primarily controlled by the recharge and discharge mechanisms. Knowing how weather and surroundings affect groundwater level is a key to measuring it accurately. Moreover, by integrating the measurements, forecasting techniques, and groundwater management strategies, a potent decision-making tool can be developed (Lerner and Harris, 2009; Shankar et al., 2011; Mishra et al., 2018; Rodell et al., 2009).

Prediction of GWL has been the subject of numerous studies utilizing various simulation techniques (Tao et al., 2022). A diverse range of stand-alone Machine Learning (ML) algorithms has been proposed and utilized for simulating GWL (Singh et al., 2024b). These algorithms encompass various forms of Artificial Neural Network (ANN) (Lallahem et al., 2005), Support Vector Machine (SVM) (Zhou et al., 2017),

* Corresponding authors.
E-mail addresses: vipul18@iiserb.ac.in (V. Bhadani), sabhilash@iiserb.ac.in (A. Singh), vaibhav@iiserb.ac.in (V. Kumar), kgaurav@iiserb.ac.in (K. Gaurav).

[1] Authors contributed equally.

https://doi.org/10.1016/j.envsoft.2024.105995
Received 25 September 2023; Received in revised form 15 January 2024; Accepted 20 February 2024
Available online 21 February 2024
1364-8152/

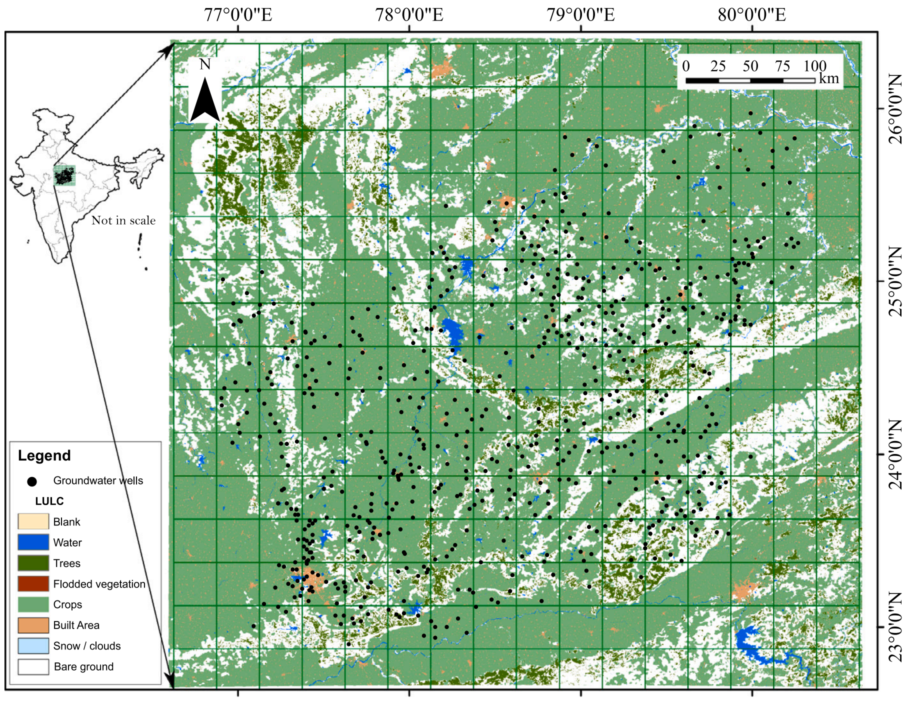

Fig. 1. Land Use and Land Cover map of the Betwa River basin (source: ESRI). Circles in black show the location of groundwater monitoring wells.

tree-based (Davoudi Moghaddam et al., 2020), and fuzzy-based models (Nadiri et al., 2019). The adoption of state-of-the-art ML models, such as Deep Learning (DL) as highlighted by Afzaal et al. (2019), extreme ML, proposed by Alizamir et al. (2018), and Long Short-Term Memory (LSTM), as described by Bowes et al. (2019), contribute to the development of new methods for estimating GWL. Several new approaches have been proposed to enhance GWL modeling, such as the implementation of hybrid ML models (Pham et al., 2019), and ensemble learning strategies (Nguyen et al., 2020). These data-driven models use GWL time series, along with meteorological and hydrological variables such as; rainfall, humidity, temperature, and evaporation, to predict the GWL (Tao et al., 2022). However, the use of Land-Use/Land-Cover (LU/LC) information remains largely unexplored in the prediction of GWL. A comprehensive survey by Tao et al. (2022) highlights the effectiveness of conventional ML methodologies such as ANN, SVM, Adaptive Neuro-fuzzy Inference Systems (ANFISs), and GP in predicting and forecasting GWL across diverse geological and climatic regions. However, it is important to note that many of these studies have utilized limited wells, typically less than 100, which may introduce bias and limit the generalizability of the results. Therefore, training the models with the data from more number of wells is crucial to developing a more reliable mapping function that accurately captures the dynamics of the processes involved.

It has been observed that the hybrid ML algorithms exhibit greater accuracy than their standalone counterparts (Tao et al., 2022; Ardabili et al., 2020; Pham et al., 2019). For instance, Dash et al. (2010) proposed a hybrid model that couples ANN with a Genetic Algorithm (GA) to accurately predict the GWL in the lower Mahanadi river basin of Orissa State, India. In a recent study, Kombo et al. (2020) proposed a hybrid ML model that combines the K-Nearest Neighbor (KNN) and Random Forest (RF) algorithms for GWL prediction. Building upon this work, Wei et al. (2022) proposed two additional hybrid algorithms that integrate SVM and RF with Wavelet Transform (WT). These studies lack handling of uncertainty and imprecision in data. Such limitations can be largely addressed by using fuzzy logic (Singh et al., 2024a; Roy et al., 2021). For example, Roy et al. (2020) utilized the FAO-56 Penman-Monteith method and ANFIS to forecast evapotranspiration in Bangladesh and South Florida. They used four nature-inspired optimization algorithms to fine-tune ANFIS. Recently, Safari et al. (2020) explored the application of the "non-deposition with deposited bed" (NDB) concept for designing large channels using hybrid ML algorithms. Initially, they developed a standalone ANFIS model, followed by hybridization with IWO and classical GA. Roy and Datta (2017a) used a Sugeno-type FIS with FCM clustering to predict salinity concentrations in coastal aquifers influenced by groundwater pumping. They trained and validated the FIS using FEMWATER simulations, reporting its capability to forecast salt concentrations at monitoring locations. Building on this, Roy and Datta (2017b) introduced a GA-tuned FIS hybrid model for regional-scale saltwater intrusion management in coastal aquifers. The GA optimizes FIS parameters, coupled with the Controlled Elitist Multi-objective Genetic Algorithm (CEMGA), enhancing the effectiveness of pumping strategies. Comparative evaluation against an ANFIS model underscores the superiority of the GA-FIS-CEMGA-based approach in efficiently controlling saltwater intrusion in a multi-layered coastal aquifer system. We found only a few studies on the application of hybrid ML and fuzzy logic together in predicting GWL (Zare and Koch, 2018; Jafari et al., 2020; Navale and Mhaske, 2022). This study proposes an integrated approach based on fuzzy logic with nature-inspired algorithms to predict GWL variations in the Betwa River basin (Fig. 1). It is located in a semi-arid climate zone in central India. The total area of the basin is approximately 44,000 km^2. It includes nine districts in Madhya Pradesh (Ashoknagar, Chhatarpur, Bhopal, Raisen, Lalitpur, Sagar, Sehore, Shivpuri, and Vidisha) and five districts in Uttar Pradesh (Tikamgarh, Mahoba, Jhansi, and Hamirpur). The Betwa River originates from the Raisen district of Madhya Pradesh and flows southwest-to-northeast until it merges with the Yamuna River near Hamirpur in Uttar Pradesh (Kumar et al., 2023). The elevation in the basin ranges from 76 to 715 meters above Mean Sea Level (MSL).

2. Material and methods

2.1. Datasets

To setup the machine learning model we used the climate, soil type, landuse/landcover, and groundwater level data of the study area.

We have downloaded rainfall, temperature, evaporation, and relative humidity for a period between 1997–2018 from the ERA-5 reanalysis dataset from the Climatic Data Store.[2] These products are available on daily time scale at grid resolution $0.25° \times 0.25°$.

To capture the seasonal variability, we categorized these datasets into pre-monsoon, monsoon, and post-monsoon periods. The monsoon period consisted of daily data from June to September (*i.e.,* JJAS), the pre-monsoon period included data from February to March, and the post-monsoon period comprised from October to January. For seasonal precipitation and evaporation, we aggregated the daily data within each period by summing them.

The soil type data is available on the Climatic Data Store. We aquired the LULC of the study area from Esri, Microsoft, and Impact Observatory prepared from Sentinel-2 at the spatial resolution of 10×10 meters.[3]

We obtained the in-situ measurement of groundwater level (1997–2018) from the Central Ground Water Board (CGWB), new Delhi and the Madhya Pradesh Water Resource Board (MPWRD). Our data archive consists of the measurement of water level below the ground (bgl) from 665 different wells distributed throughout the study area (Niranjannaik et al., 2022). The CGWB regularly collects well data during four specific months: January, May, August, and October. To synchronize with the seasonal framework, we mapped the data collection periods with the corresponding seasons. For example, the GWL data collected in May was considered as a representative value for the pre-monsoon period. Similarly, the GWL data collected in August was classified as a representative value for the monsoon period. We calculated the average of the GWL values obtained in October and January to represent a single value for the post-monsoon period.

To compute the GWL lag, we utilized the data from the previous season. The GWL data from the pre-monsoon period of a given year was used as the GWL lag for the subsequent monsoon season. The GWL data from the monsoon period served as the GWL lag for the post-monsoon period, and the GWL data from the post-monsoon period represented the GWL lag for the subsequent pre-monsoon season in the following year. This approach enabled us to consider the temporal relationships and transitions between seasons when evaluating the dynamics of GWLs.

During the pre-processing stage of the well's data points across each grid, we incorporated the impact of LULC by utilizing its information to assign representative values. By associating each well with its corresponding LULC class, we determined the class with the highest count within a specific grid. The average GWL of all wells belonging to this predominant class within the grid was considered the representative GWL for that particular grid. Using the gridded data approach in the study area, we identified a total of 126 grids that contained at least one well. We collected data covering the period from 1997 to 2018 for each of these grids. The dimensions of the final processed dataset are 8310×7 (rows $\times$ columns), where the first number indicates the total number of observations, and the latter indicates the number of input features (six) and the response variable.

2.2. Methodology

2.2.1. Feature importance

The importance of features is crucial in accurately predicting the desired output of a model. By prioritizing the most significant features we can build precise and efficient models. Additionally, considering feature importance helps to mitigate the risk of overfitting and provides valuable insights into the underlying factors influencing the outcome. We evaluated the relevance (*i.e.,* the importance scores) of input features by leveraging regression ensemble tree technique (Singh and Gaurav, 2023; Singh et al., 2023b,a,c). We utilized the Least Squares Gradient Boosting (LSBoost) technique, employing a learning rate of one, denoted as $\gamma = 1$. The boosting process involved a total of 500 regression trees, represented by $m = 500$. We employed a cross-validation technique to find the optimal number of trees (Fig. 2). This involves splitting the data into multiple folds, training the model on all the training folds, and evaluating its performance on the held-out fold (*i.e.,* the validation fold). This process was repeated for each fold, and the average MSE across all folds was calculated for each number of trees. The optimal number of trees was elected as the one that yielded the lowest average MSE across all folds. This approach prevent overfitting by assessing the performance of model on unseen data during training.

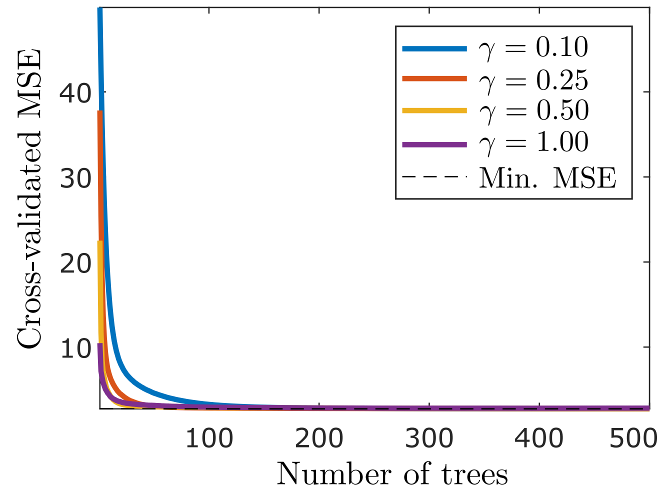

Fig. 2. Cross-validated MSE plotted as a function of the number of regression trees.

Our analysis regarded conventional decision trees, specifically decision stumps, as inadequate learners. The LSBoost algorithm trains one poor learner at a time, sequentially identifying and addressing its weaknesses. It then generates a new poor learner (l_i) based on the identified weaknesses and computes the corresponding weight (δ_i) for that learner. Finally, using Eq. (1) (Breiman et al., 1984), the method updates the current model (M_i) by addressing the specific issues identified by the previous poor learner (M_{i-1}).

$$M_i = M_{i-1} + \gamma \cdot \delta_i \cdot l_i \qquad (i = 1, 2, 3, \ldots, m) \tag{1}$$

During training, the LSBoost algorithm constructs an ensemble of poor learners, gradually forming a strong learner denoted as M_m. Each poor learner is integrated into the existing model, creating the ensemble. Subsequently, we evaluate the node risk changes resulting from splitting each feature and normalize them based on the sum of branch nodes (referred as $Risk_{branch}$). We utilize the available information to quantify each feature's relative relevance score. Eq. (2) (Breiman et al., 1984) is used to calculate the changes in node risk ($\Delta Risk$). These changes provide valuable insights into the contribution of each feature to the overall model performance and guide us in assessing their relative importance.

$$\Delta Risk = \frac{Risk_p - (Risk_{c1} + Risk_{c2})}{Risk_{branch}} \tag{2}$$

where $Risk_p$ represents the risk associated with the parent node, while $Risk_{c1}$ and $Risk_{c2}$ represent the risks of the two child nodes. At each individual node, the node risk ($Risk_i$) is calculated using Eq. (3) (Breiman et al., 1984).

$$Risk_i = NP_i \cdot MSE_i \tag{3}$$

where NP_i represents the node probability, and MSE_i corresponds to the mean square error for node i.

[2] https://cds.climate.copernicus.eu
[3] https://www.arcgis.com

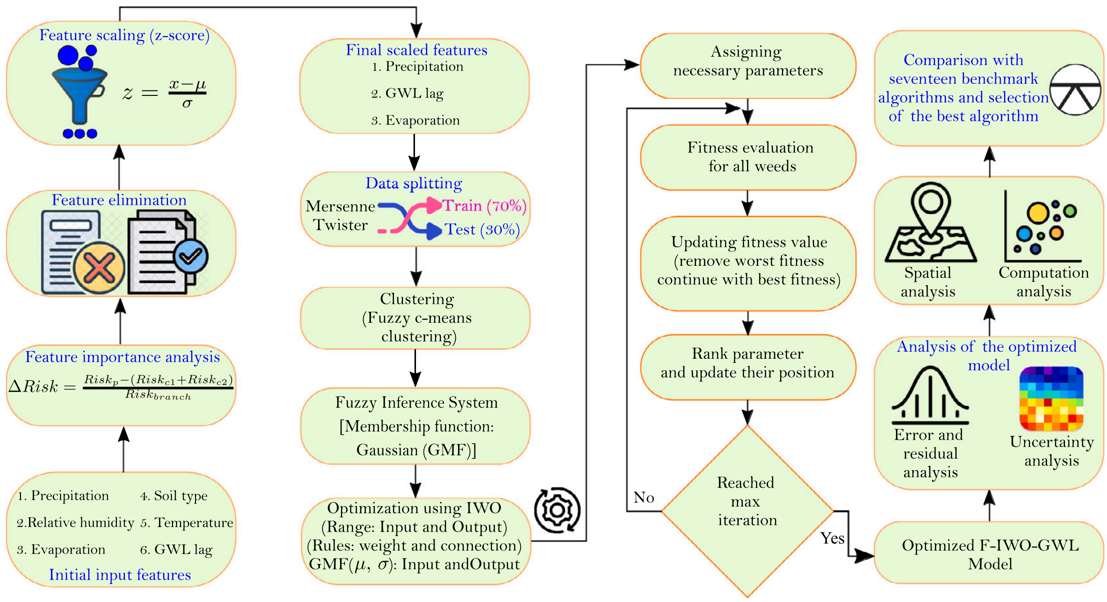

Fig. 3. Flowchart illustrating the detailed methodology for GWL prediction.

In addition, we compute a feature association matrix, which takes the form of a 6 × 6 matrix, to evaluate the correlation among the features. The presence of correlated features can harm the performance of the ML model by introducing instability and increasing sensitivity to uncertainty (Singh et al., 2021b; Nagar et al., 2023). The values within the matrix indicate the level of similarity between the decision rules based on each observation. A higher value assigned to a pair of features indicates a stronger correlation between them. After analyzing the feature importance and associations, we standardized the entire dataset using the z-score scaling approach. Following this, we divided the data into a 70:30 ratio for training and testing the proposed ML model, utilizing the Mersenne Twister random generator (Matsumoto and Nishimura, 1998). After splitting, the training and testing datasets have a dimension of 5817 × 7 and 2493 × 7, respectively.

2.2.2. Model development

We can broadly categorize the development of the proposed F-IWO-GWL model into three main steps. In this first step, we used fuzzy clustering to identify the underlying structure in the data and generate fuzzy rules. We then use these fuzzy rules in the FIS for inference and decision-making. Finally, we used defuzzification to convert the fuzzy output into a usable form for further analysis. We used fuzzy clustering to group the data into fuzzy sets (Zadeh, 1965). In this approach, each data point is assigned a membership value to each fuzzy set, indicating the degree to which it belongs to that particular set.

FIS is a type of artificial intelligence system that leverages fuzzy logic for decision-making (Mamdani and Assilian, 1975). It consists of three key components: a fuzzy rule base, a fuzzy inference engine, and a defuzzifier. The fuzzy rule base consists of a set of rules that establish relationships between input and output. The fuzzy inference engine utilizes these rules to draw inferences about the input data. The defuzzifier then comes into play, which converts the fuzzy output from the inference engine into a clear-cut, crisp output. Defuzzification is a process of translating a fuzzy output into a crisp output. This step is crucial because fuzzy outputs are not exact but rather represent a range of potential values. It uses some form of averaging to transform the fuzzy output into a single, well-defined, crisp value.

To begin, the number of clusters for the FIS (Sugeno type) is determined by considering the data characteristics and leveraging domain expertise (Sugeno, 1985). Through the Elbow method, we identified eight as the optimal cluster size. Subsequently, the cluster centers for each cluster are randomly initialized, and the membership values for each data point are calculated using the Gaussian membership function, defined by a range and variance. The cluster centers are then iteratively updated based on the calculated membership values. We applied the IWO algorithm with a population size of 50 for 100 iterations for the iterative update of the Gaussian membership function parameters for each cluster (Fig. 3). The IWO algorithm inspired by the behavior of invasive weeds in search and optimization processes is based on the biological principle of natural selection (survival of the fittest) (Xing et al., 2014). Weeds in agricultural fields disperse seeds and take advantage of unoccupied spaces, growing until they reach the flowering stage and produce more weeds (Mehrabian and Lucas, 2006). The ability of a flowering plant to generate weeds depends on its adaptation to the environment (Mallahzadeh et al., 2009). Once convergence is achieved, each data point is assigned to the cluster with the highest membership value. In the second step, we need to define the input and output variables for the FIS. We consider the input features and GWL as the input and output variables for the FIS, respectively. Finally, we defined the linguistic variable for each input and output variable and generated fuzzy rules given by Eq. (4) illustrating the relationship between the input and output variables.

$$\mathrm{Input}_1\mathrm{cluster\ (i)}\ \&\ \mathrm{Input}_2\mathrm{cluster\ (i)}\ \&\ \ldots\ \&\ \mathrm{Input}_n\mathrm{cluster\ (i)} \xrightarrow{\mathrm{Sugeno}} \mathrm{Output\ cluster\ (i)} \tag{4}$$

where i ranges from 1 to 8 and n represents the number of input features. We have a total of eight rules that map the input to the output through the AND fuzzy logic operator. Notably, each fuzzy rule corresponds to a specific consequence, represented by a linguistic term from the output variable. The overall procedure can be summarized as follows:

- Step 1: Fuzzify the crisp input values into fuzzy membership degrees using the optimized Gaussian membership functions obtained from the IWO algorithm.
- Step 2: Apply the fuzzy rules to the fuzzy input values to determine the activation level of each rule.
- Step 3: Aggregate the activated rules to obtain a fuzzy output set.
- Step 4: Defuzzify the fuzzy output to obtain a crisp GWL prediction.
- Step 5: Evaluate the performance of the FIS by comparing the predicted GWLs with the actual values using different performance

Algorithm 1 Pseudo code for F-IWO-GWL algorithm

```
procedure FuzzyClusteringWithIWO(data, num_clusters, max_iterations)
    Initialize cluster_centers randomly
    Initialize population with random solutions (IWO-specific)
    for iteration in 1 to max_iterations do
        Calculate membership values using Gaussian membership function
        Apply IWO algorithm to update cluster_centers (IWO-specific)
    end for
    Assign each data point to the cluster with the highest membership value
end procedure
procedure FuzzyInferenceSystem(input_data, cluster_centers)
    Initialize output variable GWL_output
    for each input feature in input_data do
        Calculate linguistic variables based on input feature
    end for
    for each cluster and its linguistic variables do
        Apply fuzzy rules to calculate intermediate output
    end for
    Aggregate intermediate outputs to get the final GWL_output
end procedure
procedure Defuzzify(GWL_output)
    Perform defuzzification
    Return the crisp GWL prediction
end procedure
procedure Main
    Load and preprocess the GWL data
    Split data into training (70%) and testing (30%) sets
    num_clusters = 8                                    ▷ Determine the optimal cluster size
    max_iterations = 100
    cluster_centers = FuzzyClusteringWithIWO(training_data, num_clusters, max_iterations)
    linguistic_variables = DefineLinguisticVariables()  ▷ Define linguistic variables for inputs and outputs
    fuzzy_rules = GenerateFuzzyRules(linguistic_variables)  ▷ Generate fuzzy rules
    Initialize lists for actual and predicted GWL values
    for each data point in testing_data do
        input_data = ExtractInputFeatures(data_point)   ▷ Extract input features
        GWL_output = FuzzyInferenceSystem(input_data, cluster_centers)  ▷ Perform FIS
        predicted_GWL.append(GWL_output)                ▷ Store predicted GWL
        actual_GWL.append(data_point.actual_GWL)        ▷ Store actual GWL
    end for
    R = CalculateCorrelationCoefficient(actual_GWL, predicted_GWL)
    nRMSE = CalculateRootMeanSquaredError(actual_GWL, predicted_GWL)
    bias = CalculateBias(actual_GWL, predicted_GWL)
end procedure
Main()
```

metrics (R, nRMSE, and bias). The pseudocode is presented in Algorithm 1.

3. Results

3.1. Feature importance and model accuracy

We ranked the input features from most significant to least based on their respective importance scores. Based on their rank, the important features are, GWL lag, relative humidity, precipitation, temperature, evaporation, and soil type (Fig. 4a). To streamline computations and enhance efficiency, we removed the less relevant features (*i.e.,* soil type, evaporation, and temperature). This process simplifies models, making them more interpretable and reducing the risk of overfitting to training data. The computational efficiency of the model is enhanced with fewer features, which is particularly valuable in large-scale or real-time applications. Additionally, removing less important features can mitigate issues such as multicollinearity, making coefficient estimates more stable. Consequently, only the top three input features were utilized to train and validate the F-IWO-GWL model. Furthermore, a feature association analysis revealed no significant correlations among the input features, thereby ensuring model stability (Fig. 4b).

Once the model is trained, we begin by feeding the training datasets into the model to compute the training accuracy. Remarkably, the model exhibited outstanding performance on the training data, yielding an R-value of 0.89, a normalized RMSE (nRMSE) of 0.24, and a bias of 0.01. However, evaluating the model solely based on its performance on the training data can lead to biased observations. Therefore, to assess the generalization capability of model, we evaluate its performance on unseen datasets. We fed the testing datasets into the model and recorded the corresponding performance metrics. The model demonstrated a similar level of performance on the unseen data, achieving an R-value of 0.89, a nRMSE of 0.18, and a bias of 0.08, as illustrated in Fig. 5. We found that the majority of the observations closely align with the regression line. This analysis enabled us to gauge the model's ability to generalize beyond the training data. To forecast the GWL, we need to input forecast data for the relevant features into the model.

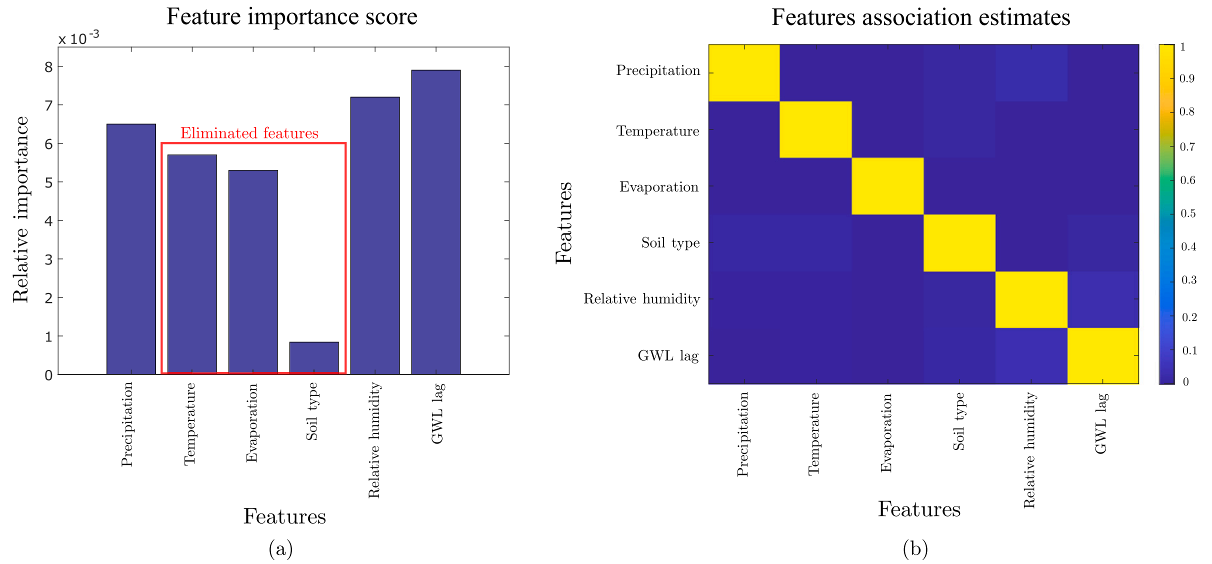

Fig. 4. (a) Bar graph shows the feature importance score of each feature and (b) Feature association matrix illustrating the correlation among each feature.

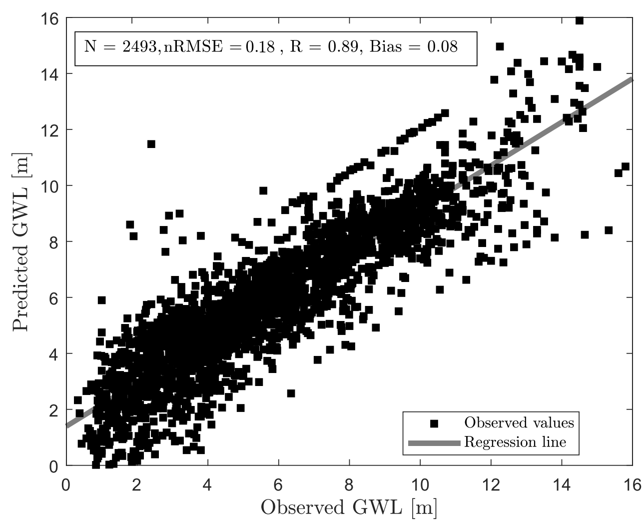

Fig. 5. Regression plot between the observed and F-IWO-GWL predicted GWL.

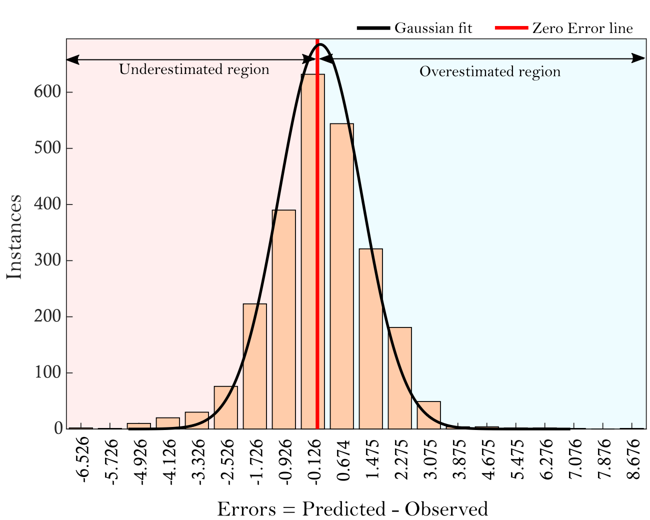

Fig. 6. Error histogram illustrating the distribution of the model error.

3.2. Error and residual analysis

An error analysis was conducted to observe and understand the error patterns, aiming to refine the model and enhance its accuracy. To achieve this, an error histogram analysis was performed. Initially, the errors were computed by subtracting the observed values from the predicted values based on the testing dataset. Subsequently, a histogram of these errors was plotted using 20 bins to examine their distribution (refer to Fig. 6). The analysis revealed that the model's error ranged from −6.53 to 8.68.

Furthermore, a Gaussian curve was fitted to analyze the distribution of errors. Notably, the peak of the error distribution precisely coincided with the zero error line, indicated by the red line. This alignment suggests our model optimally fits the data. A symmetric distribution of errors was observed, where negative errors represented the underestimated region and positive errors indicated the overestimated region. This symmetry further reinforces the robustness of the model's performance.

To assess the goodness of fit of the proposed model, we conducted a residual analysis. This involved calculating the residuals by subtracting the observed data from the fitted data generated by the model. We then plot the residuals, along with a 95% confidence interval, to visually examine their behavior (see Fig. 7). The residuals displayed a random pattern devoid of any discernible structure. This confirms their stochastic nature, indicating a strong alignment between the model's predictions and the actual observations. The absence of any systematic pattern or trend within the residuals further affirms the model's suitability and ability to capture the underlying variability in the data accurately. This also suggests that the model is not overfitting the data and that it is capturing the true underlying relationship between the variables (see Fig. 8).

3.3. Uncertainty analysis

Performing uncertainty analysis is essential for evaluating the reliability and robustness of a developed model. To accomplish this, we introduced minor uncertainties of ±5% and ±10% in each input feature while maintaining all other features constant (Fig. 8). Through the examination of the resultant changes, we gained insights into the model's response to variations in input.

We quantified the output variation of model and reported the mean percentage change (refer to Table 1). Our model exhibits a variation ranging from −6.8 to 6.9% for small uncertainties in the input features.

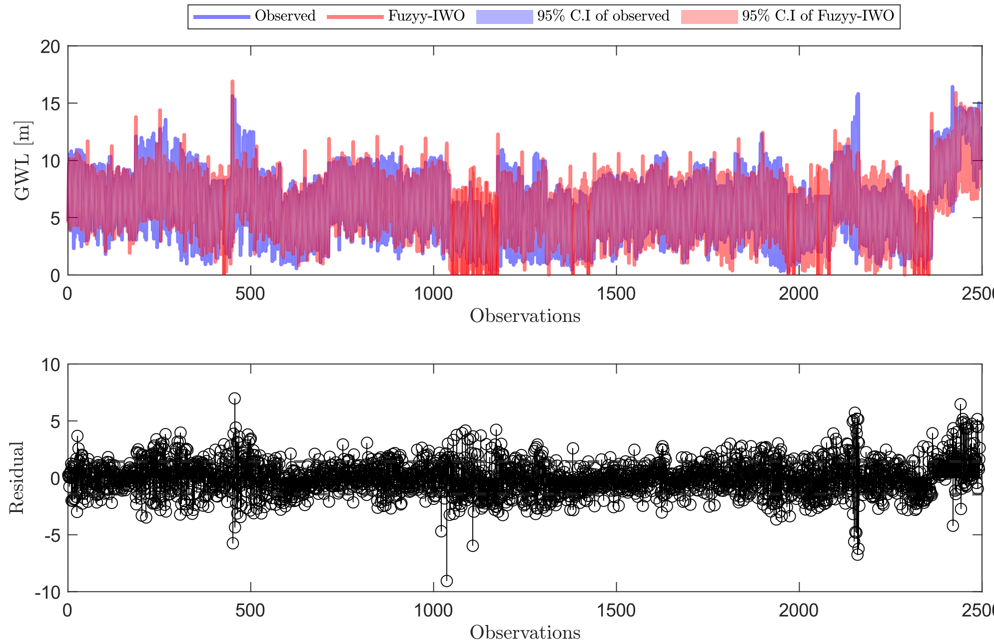

Fig. 7. Residual plot of the proposed F-IWO-GWL algorithm.

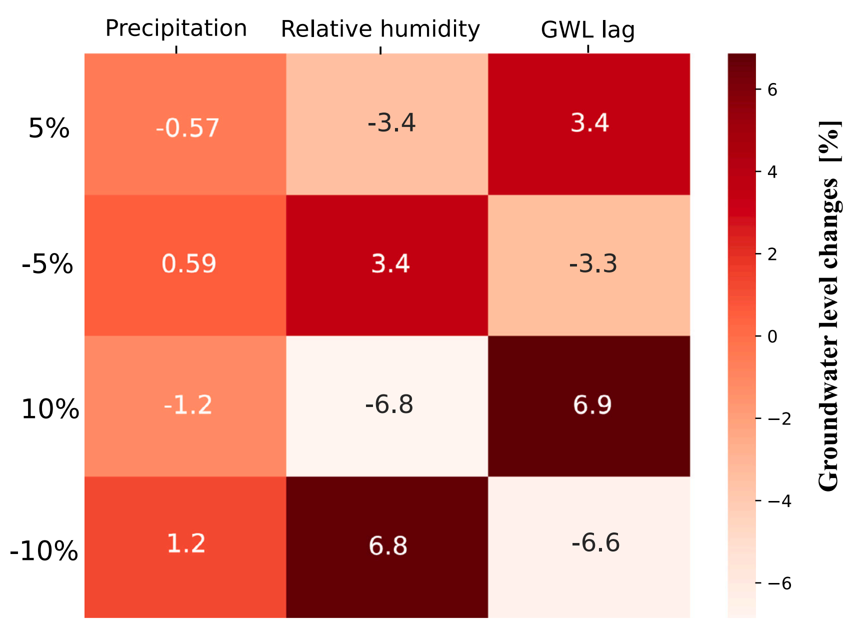

Fig. 8. Heatmap illustrating uncertainty results of the proposed F-IWO-GWL model.

Notably, the input features most affected by these uncertainties were relative humidity and GWL lag, indicating their significant relevance in the model's predictions. In comparison, precipitation displayed lower variation, suggesting its relatively lesser influence compared to GWL lag and relative humidity. Overall, the suggested F-IWO-GWL model demonstrated commendable stability in response to uncertainties in the input data. The analysis suggests that the model can produce consistent and reliable outputs, even with small fluctuations in the input variables.

4. Discussions

4.1. Spatial distribution analysis

Spatial distribution analysis is important for understanding the geographical trends and patterns in the model's response. By performing the spatial distribution of the proposed model, we can identify regions with high or low values and assess any potential spatial autocorrelation. It enables us to scrutinize the data's dependency on local

Table 1
Training and testing accuracy for different sets of datasets. 'n' represents the seed used in the random generator to generate distinct sets of training and testing datasets.

rng(n)	Training			Testing		
	nRMSE	R	Bias	nRMSE	R	Bias
n=0	0.24	0.89	0.01	0.18	0.89	0.08
n=1	0.26	0.88	0.01	0.19	0.86	0.28
n=2	0.25	0.88	0.00	0.23	0.87	−0.09
n=3	0.25	0.88	−0.01	0.22	0.87	−0.09
n=4	0.25	0.89	−0.02	0.20	0.89	−0.06
n=5	0.25	0.88	0.02	0.22	0.87	−0.05
n=6	0.24	0.89	0.02	0.19	0.89	0.05
n=7	0.25	0.88	0.00	0.22	0.88	−0.07
n=8	0.25	0.88	0.01	0.22	0.87	−0.08
n=9	0.24	0.89	0.00	0.23	0.85	0.05
n=10	0.24	0.89	0.00	0.18	0.89	0.10
n=11	0.25	0.88	0.01	0.21	0.88	−0.11
n=12	0.25	0.88	−0.01	0.22	0.87	−0.08
n=13	0.25	0.88	0.00	0.22	0.87	−0.08
n=14	0.25	0.88	0.02	0.21	0.88	−0.05
n=15	0.25	0.88	0.00	0.22	0.87	−0.09
n=16	0.25	0.89	0.01	0.19	0.89	0.07
n=17	0.24	0.89	−0.01	0.19	0.89	0.01
n=18	0.26	0.88	−0.01	0.22	0.83	0.16
n=19	0.25	0.88	0.00	0.22	0.87	−0.09
n=20	0.24	0.89	−0.01	0.17	0.89	0.16
n=21	0.25	0.88	−0.01	0.21	0.88	−0.12
n=22	0.25	0.88	0.00	0.22	0.88	−0.12
n=23	0.25	0.88	0.00	0.22	0.87	−0.08
n=24	0.25	0.88	0.00	0.20	0.88	0.01
n=25	0.25	0.88	−0.01	0.22	0.88	−0.13
n=26	0.25	0.88	0.00	0.22	0.87	−0.08
n=27	0.25	0.88	0.00	0.20	0.88	−0.02
n=28	0.24	0.89	−0.01	0.20	0.88	0.01
n=29	0.25	0.89	−0.02	0.19	0.89	−0.11
$\mu \pm \sigma$	0.25 ± 0.04	0.88 ± 0.01	0.00 ± 0.01	0.21 ± 0.01	0.88 ± 0.01	−0.02 ± 0.10

Table 2
Comparison of the F-IWO-GWL results with standalone explainable benchmark algorithms.

Performance metrics	Random Forest	Boosting Ensemble learning	Binary Decision Tree	Logistic Regression	Kernel Regression	SVR	GAM	F-IWO-GWL
R	0.88	0.83	0.80	0.87	0.79	0.88	0.88	0.89
nRMSE	0.22	0.26	0.27	0.22	0.18	0.22	0.19	0.18
Bias	0.88	0.12	0.15	−0.08	0.22	−0.06	0.07	0.08
AIC	1.40E+03	2.60E+03	2.91E+03	1.94E+03	1.33E+03	1.71E+03	1.36E+03	1.31E+03
BIC	1.43E+03	2.64E+03	2.92E+03	1.96E+03	1.35E+03	1.72E+03	1.38E+03	1.32E+03
AICc	3.90E+03	5.11E+03	5.40E+03	4.43E+03	3.84E+03	4.20E+03	3.89E+03	3.81E+03

factors, including topological, geometric, and geographic properties. Ideally, the model should demonstrate spatial independence. To assess the model's spatial stability, we used a Merseme Twister random generator (Matsumoto and Nishimura, 1998) to generate 30 distinct training and testing sets. Each case utilized a different seed, ensuring variability in the datasets. Table 1 presents the results of the suggested F-IWO-GWL model across all 30 datasets, showcasing the training and testing accuracy.

Remarkably, we observed minimal variation in the training and testing accuracy across the different datasets. This consistency indicates that our model exhibits spatial stability, with its performance remaining robust and reliable across diverse spatial contexts. The results underscore the model's ability to account for spatial dependencies and reinforce its applicability in capturing and analyzing geographic trends and patterns.

4.2. Comparison with the benchmark algorithms

To rigorously evaluate the efficacy and superiority of our proposed algorithm in predicting GWLs, we conducted a comprehensive comparative analysis against 17 benchmark algorithms. These benchmarks encompass seven standalone explainable models, five DL architectures, and five novel hybrid algorithms. The standalone explainable models in our assessment encompass a range of techniques, including RF (Breiman et al., 1984), Boosting Ensemble Learning (BoostEL) (Zhang and Ma, 2012), Binary Decision Tree (BDT) (Laurent and Rivest, 1976), Logistic Regression (LR) (Cox and Oakes, 1984), Kernel Regression (KR) (Hollander et al., 2013), Support Vector Regression (SVR) (Drucker et al., 1996), and Generalized additive model (GAM) (Hastie and Tibshirani, 1987). Within DL, we considered Generalized Regression Neural Network (GRNN) (Specht et al., 1991), ANN (Hassoun, 1995), Radial Basis Neural Network (RBNN) (Lowe, 1989), Enhanced RBNN (Broomhead and Lowe, 1988), and LSTM (Gers et al., 2000) as the key representatives. Furthermore, our evaluation extended to hybrid algorithms, where we explored combinations of FIS with various optimization techniques like Ant Colony Optimization (ACO) (Dorigo et al., 1999), Teaching-Learning-Based Optimization (TLBO) (Rao et al., 2011), Differential Evolution (DE) (Das and Suganthan, 2010), Harmony Search (HS) (Geem et al., 2001), and Weevil Damage Optimization Algorithm (WDOA) (Mousavi and Mirinezhad, 2022). These selected benchmark algorithms have been widely adopted within the scientific community and collectively represent the current state-of-the-art in GWL prediction.

To conduct a fair assessment, we trained all these benchmark algorithms using the same datasets and rigorously evaluated their performance metrics (R, nRMSE, and bias) on dedicated testing datasets,

Table 3
Comparison of the F-IWO-GWL results with deep learning benchmark algorithms.

Performance metrics	GRNN	ANN	RBNN	Enhance RBNN	LSTM	F-IWO-GWL
R	0.86	0.75	0.44	0.28	0.80	0.89
nRMSE	0.28	0.39	0.41	0.51	0.21	0.18
Bias	0.48	0.60	0.03	31.40	0.49	0.08
AIC	1.91E+03	4.96E+03	1.15E+04	1.13E+05	5.47E+03	1.31E+03
BIC	1.92E+03	5.25E+03	2.21E+04	2.82E+05	5.51E+03	1.32E+03
AICc	4.41E+03	7.46E+03	2.38E+04	5.18E+04	1.12E+04	3.81E+03

Table 4
Comparison of the F-IWO-GWL results with hybrid benchmark algorithms.

Performance metrics	F-TLBO-GWL	F-ACO-GWL	F-HS-GWL	F-DE-GWL	F-WDOA-GWL	F-IWO-GWL
R	0.87	0.88	0.88	0.81	0.88	0.89
nRMSE	0.26	0.27	0.27	0.32	0.27	0.18
Bias	0.07	0.06	0.06	−0.05	0.07	0.08
AIC	2.30E+03	2.65E+03	2.99E+03	2.13E+03	2.27E+03	1.31E+03
BIC	2.33E+03	2.68E+03	3.02E+03	2.16E+03	2.30E+03	1.32E+03
AICc	4.79E+03	5.15E+03	5.49E+03	4.63E+03	4.76E+03	3.81E+03

as detailed in Tables 2–4. In addition to conventional metrics, which are typically effective for assessing individual model performance, various other indices have been used in the literature for unbiased selection in the case of multi-model comparison (Claeskens et al., 2008; Vrieze, 2012; Singh et al., 2021a; Roy and Datta, 2020; Mattar et al., 2022). In this study, we extended our evaluation to include Akaike's Information Criterion (AIC), Bayesian Information Criterion (BIC), and Corrected AIC (AICc) for an unbiased assessment of the top-performing algorithm (Claeskens et al., 2008; Vrieze, 2012; Singh et al., 2021a). AIC, BIC, and AICc penalize the model with higher parameter counts. Therefore, the model with the lowest values for AIC, BIC, and AICc is preferred, as these metrics signify superior goodness-of-fit. This systematic comparison enables us to effectively assess whether the proposed algorithm offers significant improvements or advantages over existing methods. Our findings demonstrate that the proposed algorithm consistently outperforms all benchmark algorithms, displaying the highest R, lowest nRMSE, minimal bias, and the lowest values for AIC, BIC, and AICc. Furthermore, we conducted an evaluation and comparison of the computational time of F-IWO-GWL, contrasting it with the benchmark algorithm (Fig. 9). Our findings reveal that the F-IWO-GWL model demonstrates the lowest computation time among the evaluated models. This efficiency can be attributed, in part, to the incorporation of FCM clustering. This technique enhances computational efficiency by capturing and grouping similarities in seasonal GWL data. The integration of FCM clustering allows the development of a streamlined model based on the clustered data, contributing to the observed reduction in computation time. This striking performance disparity not only underscores the excellence of our proposed approach but also underscores its robust validity, practicality, and utility in real-world applications.

4.3. Comparison with previous studies

We conducted a comprehensive analysis by comparing the outcomes of F-IWO-GWL with recent studies to ensure a thorough evaluation. Our assessment encompassed key factors such as the number of wells, the efficacy of various algorithms, and performance metrics including the Nash–Sutcliffe model Efficiency (NSE) coefficient, R, RMSE/nRMSE, and bias (Table 5). This rigorous approach allowed for a valid and insightful comparison. In our investigation, we observed that the R values typically fell within the range of 0.64 to 0.96, while RMSE/nRMSE values varied from 0.33 to 19.0. Notably, the pivotal consideration was the number of wells taken into account. Previous studies predominantly focused on datasets with fewer than 100 wells, where achieving high accuracy might seem more straightforward. However, attaining precision with a substantial number of wells posed a considerable challenge. Our study addressed this gap by including a dataset comprising 665 wells. The remarkable achievement of obtaining a high R, lower nRMSE, and minimal bias underscored the exceptional performance of the proposed F-IWO-GWL methodology. This not only reinforces the robustness of our approach but also highlights its effectiveness in handling a larger and more complex well dataset.

4.4. Limitations and future work

The proposed F-IWO-GWL model demonstrates promising results in predicting GWL by utilizing GWL lag, relative humidity, and precipitation as input features. However, its performance can be further enhanced by incorporating additional input features, extracting valuable insights, and improving model accuracy. Variables such as land surface temperature, groundwater recharge rates, or geological characteristics hold the potential to provide a more comprehensive understanding of groundwater dynamics. Integrating these variables into the model could significantly improve its prediction accuracy. Future studies should address these limitations by exploring a wider range of input features and maintaining a balance between computational complexity and accuracy.

Furthermore, implementing a transfer learning framework could enhance the algorithm's applicability across diverse climatic zones, encompassing humid, sub-humid, semi-arid, and arid regions. This involves leveraging knowledge and insights gained from the algorithm's current performance in the semi-arid region. This adaptation would enable the model to generalize and produce reliable results across different climatic zones. The transfer learning methodology would allow us to utilize existing knowledge and model parameters as a foundation, which could then be fine-tuned and adjusted to accommodate the specific characteristics and dynamics of different regions. This would broaden the model's practical applicability and enhance its overall adaptability.

From an algorithm point of view, the existing approach can be enhanced by extending this framework along the context of a multi-agent meta-heuristic system (Silva et al., 2018). Various algorithms can be integrated into the current framework, with each algorithm serving as an agent to complete the common objective of finding the global optima. This extension requires the use of principles like parallelism, cooperation, and breaking down the search space into manageable parts.

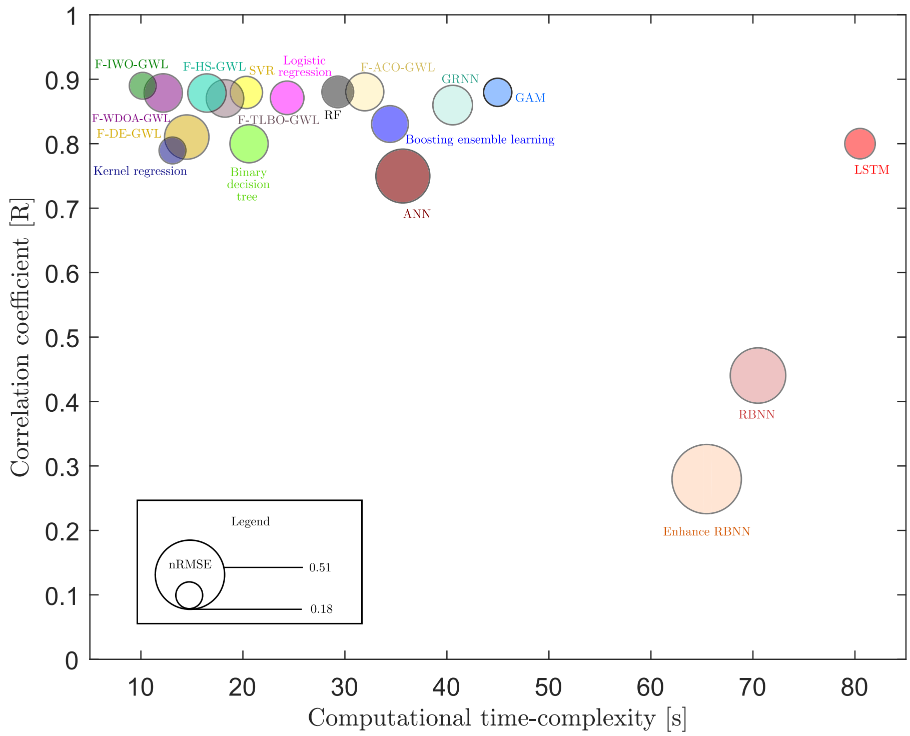

Fig. 9. Bubble plot illustrating the accuracy (R and nRMSE) and computation time of the different benchmark algorithms (each marked in a different color). The radius of the circle represents the normalized RMSE of the corresponding model.

Table 5
Comparison with recent state-of-the-art studies.

Performance metrics	Ref. Lendzioch et al. (2021)	Ref. Li et al. (2023)	Ref. Sapitang et al. (2021)	Ref. Pham et al. (2022)	Ref. Aderemi et al. (2023)	Ref. Di Nunno et al. (2023)	Ref. Zarafshan et al. (2023)	Ref. Rafik et al. (2023)	This study
N (Wells count)	63	75	10	2	20	3	24	2	665
Best performing algorithm	RF and FFS	GBR	GPR (Matern 5/2)	Bagging-RT	SVR and ANN	RBF-NN	ANFIS	RF	F-IWO-GWL
NSE	–	–	–	–	–	–	–	0.78	–
R	0.88	0.88	0.78	0.94–0.96	0.64	>0.88	0.87	–	0.89
RMSE/nRMSE	6.46	19.0	1.34	0.38–0.60	5.78	0.35–1.93	0.73	0.33	0.18
Bias	–	–	–	–	–	–	–	–	0.08

Note: RBF-NN stands for Radial basis function neural network, Bagging-RT stands for bagging regression tree, GPR stands for Gaussian process regression GBR stands for gradient boosting regression, and FFS stands for forward feature selection.

5. Conclusion

In this study, a novel regression algorithm, termed F-IWO-GWL, is proposed for accurately predicting GWL variations by taking into account the influence of LULC. The proposed algorithm seamlessly integrates FIS with a nature-inspired algorithm, offering a robust and effective GWL prediction approach. Through an extensive examination of potential input features encompassing precipitation, temperature, evaporation, relative humidity, soil type, and GWL lag, we employed regression tree ensemble learning to assess the relevance of each feature. The results unveiled that GWL lag emerged as the most significant input feature, while soil type exhibited the least relevance. To enhance the model's computational efficiency and reduce its complexity, we eliminated low-importance features such as soil type, temperature, and evaporation. The performance of the proposed F-IWO-GWL model is evaluated using a comprehensive dataset encompassing GWL measurements from 665 wells spanning the period from 1997 to 2018. This substantial dataset provides a robust foundation for training and testing the model, enabling a thorough assessment of its predictive capabilities. The evaluation results demonstrated that the F-IWO-GWL model accurately predicts GWL fluctuations with a coefficient of correlation (R) of 0.89, a normalized RMSE of 0.18, and a bias of 0.08. These impressive results highlight the model's effectiveness in capturing the intricate relationship between GWL and various environmental factors.

This research makes a significant contribution to advancing groundwater prediction techniques by introducing a reliable and robust model that enhances our understanding and management of groundwater resources. The innovative approach employed in developing the F-IWO-GWL model demonstrates substantial potential for various applications in groundwater management, including resource assessment, drought monitoring, and early warning systems. The findings provide valuable insights for policymakers and stakeholders, empowering them to make informed decisions regarding effective groundwater management strategies and policies. By effectively managing and conserving groundwater resources, we can ensure the long-term sustainability of water resources for future generations.

Funding

This work has not received any funding.

CRediT authorship contribution statement

Vipul Bhadani: Conceptualization, Data curation, Methodology, Software, Validation, Formal analysis, Investigation, Writing – original draft, Writing – reviewing & editing, Visualisation. **Abhilash Singh:** Conceptualization, Data curation, Methodology, Software, Validation, Formal analysis, Investigation, Writing – original draft, Writing – reviewing & editing, Visualisation. **Vaibhav Kumar:** Investigation, Writing – reviewing & editing, Visualisation, Supervision. **Kumar Gaurav:** Investigation, Writing – reviewing & editing, Visualisation, Supervision.

Acknowledgments

We would like to acknowledge the geohydrology observatory facility at ISERB Bhopal where the basic experiments were conducted that helped us in conceptualizing this study. AS is grateful to the Department of Science and Technology, Government of India, for funding his Ph.D. at IISER Bhopal under the DST-INSPIRE fellowship (Grant: DST/INSPIRE Fellowship/IF180001). The authors acknowledge the editor and all three anonymous reviewers for their valuable comments.

Software and data availability

- Software name: F-IWO-GWL (**F**uzzy based **I**nvasive **W**eed **O**ptimization algorithm for **G**roundwater **L**evel **P**rediction)
- Developer: Abhilash Singh
- Contact information: abhilash.singh@ieee.org
- First year available: 2024
- Program language: MATLAB
- Cost: Free
- Software availability: https://abhilashsingh.net/codes.html
- Data availability:
  - LULC data: https://planetarycomputer.microsoft.com/dataset/io-lulc
  - Input features: https://cds.climate.copernicus.eu
  - Response variable: Taken from Central Ground Water Board (CGWB) and the Madhya Pradesh Water Resource Board (MPWRD). The authors do not have permission to share this data.

Declaration of competing interest

The authors declare no conflict of interest.

References

Aderemi, B.A., Olwal, T.O., Ndambuki, J.M., Rwanga, S.S., 2023. Groundwater levels forecasting using machine learning models: A case study of the groundwater region 10 at Karst Belt, South Africa. Syst. Soft Comput. 5, 200049.

Afzaal, H., Farooque, A.A., Abbas, F., Acharya, B., Esau, T., 2019. Groundwater estimation from major physical hydrology components using artificial neural networks and deep learning. Water 12 (1), 5.

Alizamir, M., Kisi, O., Zounemat-Kermani, M., 2018. Modelling long-term groundwater fluctuations by extreme learning machine using hydro-climatic data. Hydrol. Sci. J. 63 (1), 63–73.

Ardabili, S., Mosavi, A., Várkonyi-Kóczy, A.R., 2020. Advances in machine learning modeling reviewing hybrid and ensemble methods. In: Engineering for Sustainable Future: Selected Papers of the 18th International Conference on Global Research and Education Inter-Academia–2019 18. Springer, pp. 215–227.

Bowes, B.D., Sadler, J.M., Morsy, M.M., Behl, M., Goodall, J.L., 2019. Forecasting groundwater table in a flood prone coastal city with long short-term memory and recurrent neural networks. Water 11 (5), 1098.

Breiman, L., Friedman, J.H., Olshen, R.A., Stone, C., 1984. Classification and Regression Trees. Wadsworth, Belmont, CA.

Broomhead, D.S., Lowe, D., 1988. Radial basis functions, multi-variable functional interpolation and adaptive networks. Roy. Sig. Radar Establ. Malvern (United Kingdom) 25 (3), 1–8.

Claeskens, G., Hjort, N.L., et al., 2008. Model Selection and Model Averaging, vol. 330. Cambridge University Press Cambridge.

Cox, D.R., Oakes, D., 1984. Analysis of Survival Data, vol. 21. CRC Press.

Das, S., Suganthan, P.N., 2010. Differential evolution: A survey of the state-of-the-art. IEEE Trans. Evolut. Comput. 15 (1), 4–31.

Dash, N.B., Panda, S.N., Remesan, R., Sahoo, N., 2010. Hybrid neural modeling for groundwater level prediction. Neural Comput. Appl. 19, 1251–1263.

Davoudi Moghaddam, D., Rahmati, O., Haghizadeh, A., Kalantari, Z., 2020. A modeling comparison of groundwater potential mapping in a mountain bedrock aquifer: QUEST, GARP, and RF models. Water 12 (3), 679.

Di Nunno, F., Giudicianni, C., Creaco, E., Granata, F., 2023. Multi-step ahead groundwater level forecasting in Grand Est, France: Comparison between stacked machine learning model and radial basis function neural network. Groundw. Sustain. Develop. 101042.

Dorigo, M., Di Caro, G., Gambardella, L.M., 1999. Ant algorithms for discrete optimization. Artif. Life 5 (2), 137–172.

Drucker, H., Burges, C.J., Kaufman, L., Smola, A., Vapnik, V., 1996. Support vector regression machines. Adv. Neural Inform. Process. Syst. 9.

Geem, Z.W., Kim, J.H., Loganathan, G.V., 2001. A new heuristic optimization algorithm: harmony search. Simulation 76 (2), 60–68.

Gers, F.A., Schmidhuber, J., Cummins, F., 2000. Learning to forget: Continual prediction with LSTM. Neural Comput. 12 (10), 2451–2471.

Hassoun, M.H., 1995. Fundamentals of Artificial Neural Networks. MIT Press.

Hastie, T., Tibshirani, R., 1987. Generalized additive models: some applications. J. Amer. Statist. Assoc. 82 (398), 371–386.

Hollander, M., Wolfe, D., Chicken, E., 2013. Nonparametric statistical methods. John Wiley & Sons.

Jafari, M.M., Ojaghlou, H., Zare, M., Schumann, G.J.-P., 2020. Application of a novel hybrid wavelet-ANFIS/fuzzy c-means clustering model to predict groundwater fluctuations. Atmosphere 12 (1), 9.

Kombo, O.H., Kumaran, S., Sheikh, Y.H., Bovim, A., Jayavel, K., 2020. Long-term groundwater level prediction model based on hybrid KNN-rf technique. Hydrology 7 (3), 59.

Kumar, A., Singh, A., Gaurav, K., 2023. Assessing the synergic effect of land use and climate change on the upper Betwa River catchment in Central India under present, past, and future climate scenarios. Environ. Develop. Sustain. 25 (6), 5163–5184.

Lallahem, S., Mania, J., Hani, A., Najjar, Y., 2005. On the use of neural networks to evaluate groundwater levels in fractured media. J. Hydrol. 307 (1–4), 92–111.

Laurent, H., Rivest, R.L., 1976. Constructing optimal binary decision trees is NP-complete. Inform. Process. Lett. 5 (1), 15–17.

Lendzioch, T., Langhammer, J., Vlček, L., Minařík, R., 2021. Mapping the groundwater level and soil moisture of a montane peat bog using uav monitoring and machine learning. Remote Sens. 13 (5), 907.

Lerner, D.N., Harris, B., 2009. The relationship between land use and groundwater resources and quality. Land use policy 26, S265–S273.

Li, W., Finsa, M.M., Laskey, K.B., Houser, P., Douglas-Bate, R., 2023. Groundwater level prediction with machine learning to support sustainable irrigation in Water Scarcity Regions. Water 15 (19), 3473.

Lowe, D., 1989. Adaptive radial basis function nonlinearities, and the problem of generalisation. In: 1989 First IEE International Conference on Artificial Neural Networks, (Conf. Publ. No. 313). IET, pp. 171–175.

Maiti, S., Tiwari, R., 2014. A comparative study of artificial neural networks, Bayesian neural networks and adaptive neuro-fuzzy inference system in groundwater level prediction. Environ. Earth Sci. 71, 3147–3160.

Mallahzadeh, A.R., Es' haghi, S., Alipour, A., 2009. Design of an E-shaped MIMO antenna using IWO algorithm for wireless application at 5.8 GHz. Prog. Electromagn. Res. 90, 187–203.

Mamdani, E.H., Assilian, S., 1975. An experiment in linguistic synthesis with a fuzzy logic controller. Int. J. Man-Mach. Stud. 7 (1), 1–13.

Matsumoto, M., Nishimura, T., 1998. Mersenne twister: a 623-dimensionally equidistributed uniform pseudo-random number generator. ACM Trans. Model. Comput. Simul. (TOMACS) 8 (1), 3–30.

Mattar, M.A., Roy, D.K., Al-Ghobari, H.M., Dewidar, A.Z., 2022. Machine learning and regression-based techniques for predicting sprinkler irrigation's wind drift and evaporation losses. Agricult. Water Manag. 265, 107529.

Mehrabian, A.R., Lucas, C., 2006. A novel numerical optimization algorithm inspired from weed colonization. Ecol. Inform. 1 (4), 355–366.

Mishra, V., Asoka, A., Vatta, K., Lall, U., 2018. Groundwater depletion and associated CO2 emissions in India. Earth's Fut. 6 (12), 1672–1681.

Mousavi, S., Mirinezhad, S., 2022. Weevil damage optimization algorithm and its applications. J. Fut. Sustain. 2 (4), 133–144.

Nadiri, A.A., Naderi, K., Khatibi, R., Gharekhani, M., 2019. Modelling groundwater level variations by learning from multiple models using fuzzy logic. Hydrol. Sci. J. 64 (2), 210–226.

Nagar, J., Chaturvedi, S.K., Soh, S., Singh, A., 2023. A machine learning approach to predict the k-coverage probability of wireless multihop networks considering boundary and shadowing effects. Expert Syst. Appl. 226, 120160.

Navale, V., Mhaske, S., 2022. Artificial neural network (ANN) and adaptive neuro-fuzzy inference system (ANFIS) model for forecasting groundwater level in the Pravara River Basin, India. Model. Earth Syst. Environ. 1–14.
Nguyen, P.T., Ha, D.H., Jaafari, A., Nguyen, H.D., Van Phong, T., Al-Ansari, N., Prakash, I., Le, H.V., Pham, B.T., 2020. Groundwater potential mapping combining artificial neural network and real AdaBoost ensemble technique: the DakNong province case-study, Vietnam. Int. J. Environ. Res. Public Health 17 (7), 2473.
Niranjannaik, M., Kumar, A., Beg, Z., Singh, A., Swarnkar, S., Gaurav, K., 2022. Groundwater variability in a Semi-Arid River Basin, Central India. Hydrology 9 (12), 222.
Pham, B.T., Jaafari, A., Prakash, I., Singh, S.K., Quoc, N.K., Bui, D.T., 2019. Hybrid computational intelligence models for groundwater potential mapping. Catena 182, 104101.
Pham, Q.B., Kumar, M., Di Nunno, F., Elbeltagi, A., Granata, F., Islam, A.R.M.T., Talukdar, S., Nguyen, X.C., Ahmed, A.N., Anh, D.T., 2022. Groundwater level prediction using machine learning algorithms in a drought-prone area. Neural Comput. Appl. 34 (13), 10751–10773.
Rafik, A., Brahim, Y.A., Amazirh, A., Ouarani, M., Bargam, B., Ouatiki, H., Bouslihim, Y., Bouchaou, L., Chehbouni, A., 2023. Groundwater level forecasting in a data-scarce region through remote sensing data downscaling, hydrological modeling, and machine learning: A case study from Morocco. J. Hydrol.: Reg. Stud. 50, 101569.
Rao, R.V., Savsani, V.J., Vakharia, D., 2011. Teaching–learning-based optimization: a novel method for constrained mechanical design optimization problems. Comput.-Aid. Des. 43 (3), 303–315.
Rodell, M., Velicogna, I., Famiglietti, J.S., 2009. Satellite-based estimates of groundwater depletion in India. Nature 460 (7258), 999–1002.
Roy, D.K., Barzegar, R., Quilty, J., Adamowski, J., 2020. Using ensembles of adaptive neuro-fuzzy inference system and optimization algorithms to predict reference evapotranspiration in subtropical climatic zones. J. Hydrol. 591, 125509.
Roy, D.K., Datta, B., 2017a. Fuzzy C-mean clustering based inference system for saltwater intrusion processes prediction in coastal aquifers. Water Resour. Manage. 31, 355–376.
Roy, D.K., Datta, B., 2017b. Genetic algorithm tuned fuzzy inference system to evolve optimal groundwater extraction strategies to control saltwater intrusion in multilayered coastal aquifers under parameter uncertainty. Model. Earth Syst. Environ. 3 (4), 1707–1725.
Roy, D.K., Datta, B., 2020. Saltwater intrusion prediction in coastal aquifers utilizing a weighted-average heterogeneous ensemble of prediction models based on Dempster-Shafer theory of evidence. Hydrol. Sci. J. 65 (9), 1555–1567.
Roy, D.K., Lal, A., Sarker, K.K., Saha, K.K., Datta, B., 2021. Optimization algorithms as training approaches for prediction of reference evapotranspiration using adaptive neuro fuzzy inference system. Agricult. Water Manag. 255, 107003.
Safari, M.J.S., Mohammadi, B., Kargar, K., 2020. Invasive weed optimization-based adaptive neuro-fuzzy inference system hybrid model for sediment transport with a bed deposit. J. Clean. Prod. 276, 124267.
Sapitang, M., Ridwan, W.M., Ahmed, A.N., Fai, C.M., El-Shafie, A., 2021. Groundwater level as an input to monthly predicting of water level using various machine learning algorithms. Earth Sci. Inform. 14, 1269–1283.
Shankar, P.V., Kulkarni, H., Krishnan, S., 2011. India's groundwater challenge and the way forward. Econom. Polit. Weekly 37–45.
Silva, M.A.L., de Souza, S.R., Souza, M.J.F., de Franca Filho, M.F., 2018. Hybrid metaheuristics and multi-agent systems for solving optimization problems: A review of frameworks and a comparative analysis. Appl. Soft Comput. 71, 433–459.
Singh, A., Amutha, J., Nagar, J., Sharma, S., 2023a. A deep learning approach to predict the number of k-barriers for intrusion detection over a circular region using wireless sensor networks. Expert Syst. Appl. 211, 118588.
Singh, A., Gaurav, K., 2023. Deep learning and data fusion to estimate surface soil moisture from multi-sensor satellite images. Sci. Rep. 13 (1), 2251.
Singh, A., Gaurav, K., Rai, A.K., Beg, Z., 2021a. Machine learning to estimate surface roughness from satellite images. Remote Sens. 13 (19), 3794.
Singh, A., Mehra, M., Kumar, A., Niranjannaik, M., Priya, D., Gaurav, K., 2023b. Leveraging hybrid machine learning and data fusion for accurate mapping of malaria cases using meteorological variables in western India. Intell. Syst. Appl. 17, 200164.
Singh, A., Mousavi, S.M.H., Nagar, J., 2024a. F-TLBO-ID: Fuzzy fed teaching learning based optimisation algorithm to predict the number of k-barriers for intrusion detection. Appl. Soft Comput. 111163.
Singh, A., Nagar, J., Amutha, J., Sharma, S., 2023c. P2CA-GAM-ID: Coupling of probabilistic principal components analysis with generalised additive model to predict the k- barriers for intrusion detection. Eng. Appl. Artif. Intell. 126, 107137.
Singh, A., Nagar, J., Sharma, S., Kotiyal, V., 2021b. A Gaussian process regression approach to predict the k-barrier coverage probability for intrusion detection in wireless sensor networks. Expert Syst. Appl. 172, 114603.
Singh, A., Patel, S., Bhadani, V., Kumar, V., Gaurav, K., 2024b. AutoML-GWL: Automated machine learning model for the prediction of groundwater level. Eng. Appl. Artif. Intell. 127, 107405.
Specht, D.F., et al., 1991. A general regression neural network. IEEE Trans. Neural Netw. 2 (6), 568–576.
Sugeno, M., 1985. Industrial Applications of Fuzzy Control. Elsevier Science Inc..
Tao, H., Hameed, M.M., Marhoon, H.A., Zounemat-Kermani, M., Salim, H., Sungwon, K., Sulaiman, S.O., Tan, M.L., Sa'adi, Z., Mehr, A.D., et al., 2022. Groundwater level prediction using machine learning models: A comprehensive review. Neurocomputing.
Vrieze, S.I., 2012. Model selection and psychological theory: a discussion of the differences between the Akaike information criterion (AIC) and the Bayesian information criterion (BIC).. Psychol. Methods 17 (2), 228.
Wei, A., Chen, Y., Li, D., Zhang, X., Wu, T., Li, H., 2022. Prediction of groundwater level using the hybrid model combining wavelet transform and machine learning algorithms. Earth Sci. Inform. 15 (3), 1951–1962.
Xing, B., Gao, W.-J., Xing, B., Gao, W.-J., 2014. Invasive weed optimization algorithm. In: Innovative Computational Intelligence: A Rough Guide to 134 Clever Algorithms. Springer, pp. 177–181.
Zadeh, L.A., 1965. Fuzzy sets. Inform. Control 8 (3), 338–353.
Zarafshan, P., Etezadi, H., Javadi, S., Roozbahani, A., Hashemy, S.M., Zarafshan, P., 2023. Comparison of machine learning models for predicting groundwater level, case study: Najafabad region. Acta Geophys. 71 (4), 1817–1830.
Zare, M., Koch, M., 2018. Groundwater level fluctuations simulation and prediction by ANFIS-and hybrid wavelet-ANFIS/Fuzzy C-means (FCM) clustering models: Application to the miandarband plain. J. Hydro-Environ. Res. 18, 63–76.
Zhang, C., Ma, Y., 2012. Ensemble Machine Learning: Methods and Applications. Springer.
Zhongming, Z., Linong, L., Xiaona, Y., Wangqiang, Z., Wei, L., et al., 2021. UN World Water Development Report 2021 'Valuing Water'.
Zhou, T., Wang, F., Yang, Z., 2017. Comparative analysis of ANN and SVM models combined with wavelet preprocess for groundwater depth prediction. Water 9 (10), 781.